

## MICROSYSTEM FOR BIOLOGICAL ANALYSIS BASED ON MAGNETORESISTIVE SENSING

*J. Germano*<sup>1</sup>, *M. S. Piedade*<sup>2</sup>, *L. Sousa*<sup>3</sup>, *T. M. Almeida*<sup>4</sup>, *P. Lopes*<sup>5</sup>,  
*F. A. Cardoso*<sup>6</sup>, *H. A. Ferreira*<sup>7</sup>, *P. P. Freitas*<sup>8</sup>

<sup>1,2,3,4,5</sup> INESC-ID/IST, Lisboa, Portugal, jahg@sips.inesc-id.pt, msp@inesc-id.pt, las@inesc-id.pt, tmma@inesc-id.pt, paulo.c.lopes@inesc-id.pt

<sup>6,7,8</sup> INESC-MN/IST, Lisboa, Portugal, fcardoso@inesc-mn.pt, hferreira@inesc-mn.pt, pfreitas@inesc-mn.pt

**Abstract:** This paper presents a microsystem for biomolecular recognition (DNA, enzymes) based on a biochip, which uses magnetic field arraying of magnetically tagged biomolecules and high sensitivity sensors for single biomolecule detection. The microsystem provides the electronic circuitry for addressing, reading out and sensing each of the  $16 \times 16$  magnetoresistive sensors that compose the biochip. A prototype of the microsystem was developed and experimental results show that it is able of nanoparticle detection and, consequently, be used for magnetic labelled based bioassays.

**Keywords:** microsystem, biochip, biomolecular recognition.

### 1. INTRODUCTION

Biochips are biological sensing devices used in lab-on-chip platforms to obtain higher levels of integration and, nowadays, are often used as a disposable cartridge [1]. Recently, magnetoresistive biochips have been used for integrated biomolecular recognition assays [2], using target biomolecules marked with magnetic particles.

The microsystem described in this work is based on a new type of magnetoresistive biochip, fabricated by INESC-MN using standard microfabrication techniques. Each biosensor detection site incorporates a Thin Film

Diode (TFD), p-type, intrinsic, n-type (p-i-n) or Schottky, in series with a magnetic sensor, based on a Magnetic Tunnel Junction (MTJ). The biochip is organized as a matrix of biosensor detector sites (fig. 1), actually with 256 sites, but that can be easily scaled up for a larger numbers of probes.

In fig. 1, each diode ( $D_{i,j}$ ) is used as a switching device, enabling the connection of a specific column and row of the matrix and it also acts as a temperature sensor of each biosensor site ( $B_{i,j}$ ). Each MTJ element ( $S_{i,j}$ ) is very close to the diode (fig. 1(b)) and operates as a sensor of the planar magnetic field ( $H$ ) transversal to its length.

In the microsystem proposed in this paper, the biochip is integrated in a specific miniature (credit card dimension) handheld platform incorporating all electronics for addressing, reading out, sensing and temperature control, as well as the micro fluidics chamber and control [3, 4]. High level system control and data analysis are remotely performed through a Personal Digital Assistant (PDA) via a wireless channel or an Universal Serial Bus (USB).

### 2. PLATFORM ARCHITECTURE

The proposed architecture for the biochip platform is organised in two main modules (fig. 2): *i*) the Sensing and Processing Module (SPM) and *ii*) the Fluid Control and Communications Module (FCCM). The SPM integrates the biochip and provides the circuits that directly interact with the array of biosensors (biochip), in order to individually address sensors, readout data from them and to control the temperature in the different sub-areas of the biochip. The FCCM interfaces the platform with the external world, by controlling the fluid carrying the magnetically tagged biomolecules and providing wireless communication with a handheld analyser, based on a PDA. The handheld device acts as the master of the system, giving the geneticist/biologist the biological measures.

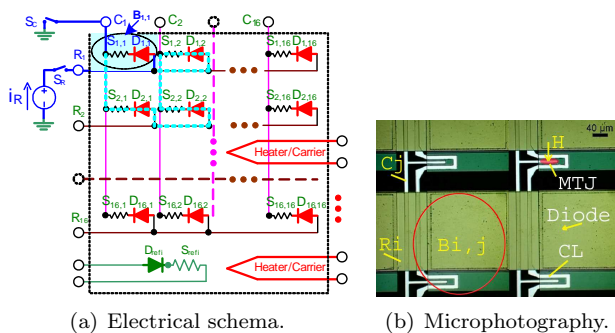


Figure 1: Magnetoresistive biochip.

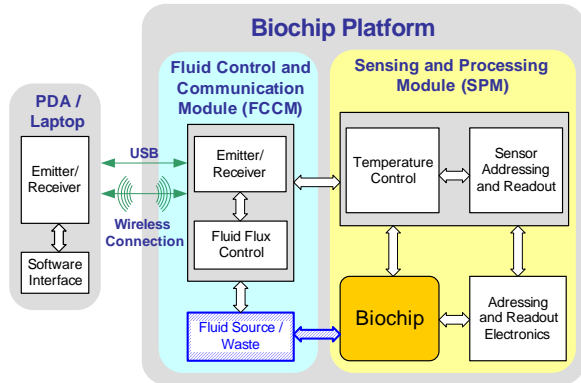


Figure 2: Biochip platform architecture.

### 2.1. Sensing and processing

Sensor addressing is based on a commutating matrix of integrated diodes, each one acting as a switch in series with the corresponding MTJ magnetoresistive sensor. A single element is addressed by operating a demultiplexer, to connect the programmable current source to a row of sites (diode in series with MTJ), and a multiplexer, for addressing the column to be connected to the ground, in order to establish a single current path. The microcontroller provides the row/column address of the sensor to be read. Figure 3 depicts the adopted architecture for both addressing and sensor driving. Using a current

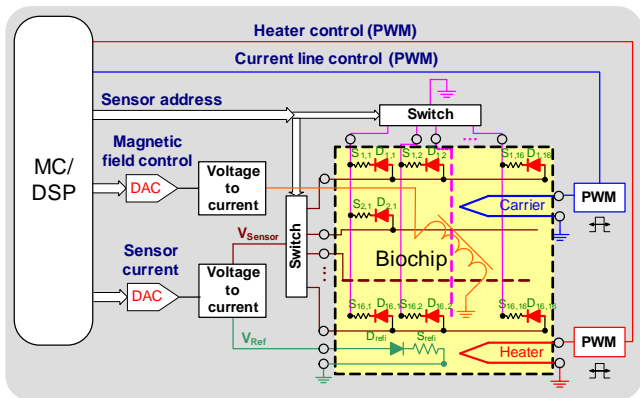


Figure 3: Addressing and sensor drive.

generated through a Digital to Analog Converter (DAC) ensures high flexibility as arbitrary waveforms can be generated. For the sensor structure operation it is always required to provide a DC current to polarize the diode. Furthermore, a possible method for sensor reading consists on driving the sensor structure with a DC current superimposed to a AC component. A current mirror circuit also provides a current with equal value for a similar sensor structure ( $D_{ref}$  and  $S_{ref}$  placed on specific locations of the chip) used to provide reference values. Another way of performing a measure is to provide a DC current to polarize the diode and use an external magnetic field for varying the sensor resistance.

Hence, a circuit was developed capable of generating an oscillating magnetic field. This can be created by applying a current to an external coil and controlling the current using a DAC with output in current.

As the temperature of the biochip must be controlled, there are heaters placed in different areas of the chip capable of providing a considerable amount of thermal power. Control is made by applying Pulse Width Modulation (PWM) signals. The biochip has current lines (*Carrier* in fig. 3) to guide the magnetic particles over the magnetic sensor [5]. These lines can be operated using a similar PWM controller and a driver.

### Signal acquisition

The sensor is driven by a current source and the sensor resistance can be determined by acquiring the voltage drop at its terminals (fig. 3,  $V_{Sensor}$ ). The signal is acquired by using a single instrumentation amplifier and just one Analog to Digital Converter (ADC) to all the sensor elements in the array.

The same circuit is simultaneously used to sense the temperature at each site, by using the  $V(T)$  characteristic of the fabricated diodes [6]. The gain of the amplifier has to be programmable and the ADC provides the digital values to the MicroController/Digital Signal Processor (MC/DSP). Reference and source signal have to be placed at the input of the differential amplifier. Moreover it has to accept signals with or without the DC component and to be able to consider different references, such as: the ground reference, a signal from the reference sensor or a calibration value provided by the MC/DSP through a DAC. The usage of a calibration value provided by the MC/DSP allows to use the sensor as a reference for itself.

### Signal processing and control

The MC/DSP is the programmable core of the platform, operating stand-alone but with an interface for communicating with a handheld analyzer (see fig. 2). Its main tasks are: *i)* to control the operation of the reading out circuits; *ii)* to make an initial calibration of the sensors; and *iii)* to implement the signal processing and the temperature control algorithms.

In practice, the MC/DSP is a microprocessor with a Reduced Instruction-Set Computer (RISC) architecture but suitable for control, supporting an Instruction Set Architecture (ISA) that includes instructions for testing and manipulating individual bits and with a rich set of timers and powerful peripherals. At the same time, the MC/DSP has to provide dedicated hardware and instructions specific for digital signal processing in real time. This MC/DSP is programmed and configured by nonvolatile, rewritable memory and also includes a considerable amount of external volatile Random Access Memory (RAM) for storing the acquired and processed data to be transmitted to a handheld analyzer.

The temperature sensors are calibrated by programming the digital processor to generate current pulses modulated in PWM. The calibration is performed in DC, and occurs at setup time, in order to experimentally extract the diode parameters that allows to relate voltage with temperature. Calibration tables are filled for each sensor with the absolute and the differential voltages measured using reference sensors available on the chip. Filtering, equivalent lock-in amplification, sensor calibration and control algorithms are operations programmed in the MC/DSP. Programs have been developed to characterize each cell from the point of view of magnetic and temperature sensitivities and nonlinearities. At the end, the automatic individual sensor calibration will allow the counting of labels, which means target biomolecules over each sensor.

## 2.2. Communication module and handheld analyser

This module is also responsible with the interface between the biochip platform with the exterior world, typically using a PDA or a laptop. To achieve a reliable and flexible architecture, the module includes a wired and also a wireless communication module. This emitter/receiver uses the USB protocol, and also provides radio frequency for short range communication, by using Bluetooth technology (2.4 GHz). Command and data are transmitted through the serial channel and the analyzer can also be used as a data-logger, storing raw data or processed data that can be used in future experiments for comparison purposes.

At the top of the portable system, is the handheld analyzer that provides an interface to the user, allowing a user friendly interaction with the biochip platform. The defined architecture is designed to indistinctly use a PDA or a laptop to implement the handheld analyzer. All the software to analyze data, to implement the user interface and to control the overall operation of the biochip platform is being developed by using object oriented paradigm and compilers. Only the user interface is dynamically adjustable according to the characteristics of the device.

## 3. PROTOTYPE

A prototype of the system was implemented based on the architecture proposed in the previous section. The presented implementation, corresponding to a small autonomous handheld platform, is depicted in fig. 4. A modular design is adopted with the two modules implemented into two independent Printed Circuit Boards (PCBs): a main board, where the biochip is installed along with all the electronic for driving and reading the sensors; and an auxiliary board with the fluid flux control and the interface for communicating with the PDA.

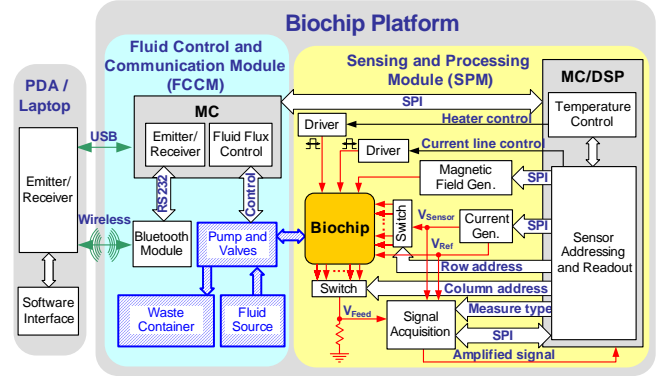


Figure 4: Diagram of the adopted function arrangement.

### 3.1. Reading and controlling circuits

The core of the system is a 16-bit integrated microcontroller (MC/DSP), the Microchip dsPIC 30F6014, capable of performing up to 30 Million Instructions Per Second (MIPS) and exhibiting an extended instruction set for digital signal processing [7]. A Static Random Access Memory (SRAM) is also in the SPM, providing an additional memory space that can be used to store the acquired samples or calibration data extracted from the biochip. The MC/DSP communicates with a microcontroller in the auxiliary board through the Serial Peripheral Interface (SPI), and it is programmed to perform a set of pre-defined tasks, according to the commands received from the PDA. This MC/DSP addresses and reads the data from the array of magnetoresistive sensors provided by the biochip and it measures and controls the temperature by using the same devices. To perform all these operations, the MC/DSP controls the circuits that are represented in fig. 4 and described in the next subsections.

#### Current generator circuits

To read the complete sensor array, the required current is generated using a DAC and a voltage-to-current converter and is multiplexed into the biochip, allowing the usage of only one current generator. Figure 5 depicts the circuit diagram employed in the current generator. The DAC voltage output is converted to current by using a non inverting amplifier topology with a NPN transistor ( $Q_{Feed}$ ) and a resistor. Two current mirrors are implemented to guarantee that a current with equal value is injected in the reference sensor. The  $R_e$  resistor in the current mirror introduces negative series-series feedback and increases the circuit output impedance improving the circuit operation. With this topology, current errors introduced by the mirror and by the feedback transistor are reduced. The error that still remains is the offset error of the Operational Amplifier (OPAMP), but it can also be attenuated, if necessary, by using a calibration table for the different DAC. The current delivered to the sensor is defined through  $R_{Feed}$ , where  $V_{DAC}$  is the

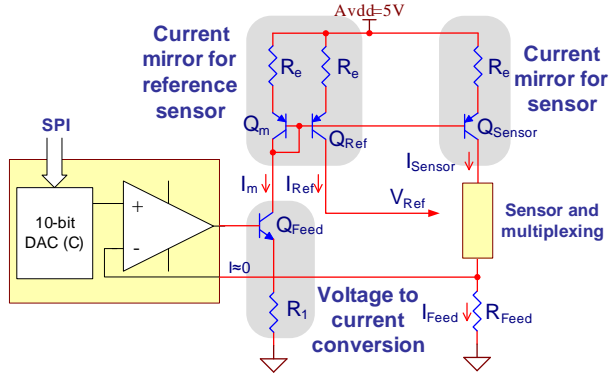


Figure 5: Current generation circuit.

DAC output voltage,  $I_{Feed} = V_{DAC}/R_{Feed}$ .

For the magnetic field generator, a circuit similar to the one used for the generation of the sensor drive current was designed. It uses a non inverting amplifier topology with a NPN transistor in the feedback loop. With this circuit, the current intensity in the coil, and consequently the magnetic field, is controlled by using the DAC and it is scaled through a resistor.

#### Carriers lines and heaters

The biochip also includes the carrier circuit to generate local magnetic fields to guide the target biomolecules over immobilised biological probes. The current required for this circuit is generated taking advantage of PWM output peripherals available on the selected MC/DSP. The only required external component is a MOS transistor, operating as a switch, and a resistor to limit the peak current. The heater circuit, that provides thermal power to the biochip, is also implemented using a PWM signal output, a transistor and a resistor. The carrier line and the heater both present a low resistance, about  $40 \Omega$ .

#### Signal acquisition circuit

The voltage across each matrix element (diode in series with the magnetic sensor) is measured using the signal conditioning circuit and the ADC. The electronic circuits for signal acquisition are represented in fig. 6.

The signals connected to the amplifier stage are defined using two switches. This circuit can provide several measurement types, including calibration measures, with two different resolution/speeds and controllable gain.

#### Signal conditioning circuit

Two switches at the input of the amplifier make possible all the measures presented in tab. 1.

Since the power source of the amplifier is not symmetric, when using the AC measures a offset must be added to the input signals after decoupling. This offset is cancelled due to the high Common-Mode Rejection Rate (CMRR) of the employed OPAMP but is required

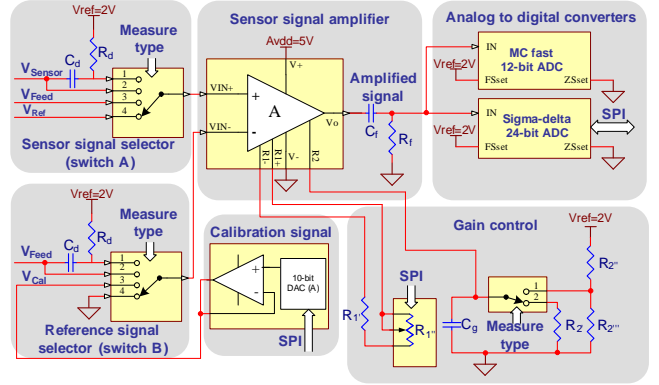


Figure 6: Circuit diagram of the sensor reading.

Table 1: Available measure schemes.

switch A	switch B	Amplified signal
1	1	$V_{AC} \text{ Sensor} - V_{AC} \text{ Feed}$
2	2	$V_{DC} \text{ Sensor} - V_{DC} \text{ Feed}$
2	3	$V_{DC} \text{ Sensor} - V_{Cal}$
3	4	$V_{Feed}$
4	4	$V_{Ref}$

to ensure the operation in the linear region. The voltage of the current source feedback resistor ( $V_{Feed}$ ) can also be acquired allowing to built a calibration table for the drive current, improving the accuracy of the circuit. The gain is set with a digital potentiometer, which is used as a rheostat controlled through a SPI interface ( $R_1$ ) and other external resistors ( $R_2$ ). Since the required gain for AC measures is very high, two different sets of resistors can be selected to provide high gain to differential measures (50 to 1000 V/V) and small gain/attenuation for the DC signal acquisitions (0.5 to 10 V/V). In the AC mode it is required to add an offset also to the output signal. This amplification block also includes a low pass filter ( $C_f$ ,  $R_f$ ) to eliminate the high frequency noise generated by the switching instrumentation amplifier.

#### Signal digitalization

The amplified signal is converted to the digital domain using a high resolution sigma-delta converter or a successive approximation faster ADC. The usage of a converter with high resolution ensures that even in DC mode, with small amplification, the target detection can be performed. This ADC can be configured using the SPI interface to several conversion speeds, but the increase in speed is paid with lower resolutions. For a conversion speed of  $880 \text{ Hz}$ , the effective resolution drops to 21 bit. The MC/DSP as a built-in 12-bit ADC that can be used to read the sensor temperature, even during the acquisition phase, when the sensor signal is converted by the high resolution low speed ADC. Another application of this converter is to make the adjustment of the amplifier gain stage. This decreases the Automatic Gain Control (AGC) adjustment time and thereby the sample acquisition time.

### 3.2. System programming

The MC/DSP must perform several tasks before making the actual reading of the biochip. The biochip reading involve the following phases: *Calibration*, *Temperature Measuring and Control* and *Signal Measuring*. Furthermore, there are several types of measures that can be selected. A full sample analysis will require the MC/DSP operations summarised by the flow chart presented in fig. 7.

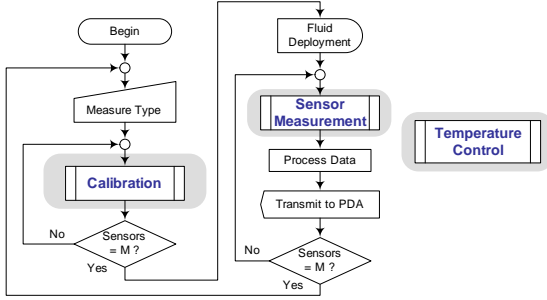


Figure 7: Sample analysis sequence.

The system is in sleep mode until a user action takes place, and a measurement type is selected and sent from the PDA to the biochip platform. After that, the system enters a first cycle in which the calibration of the platform is performed and diode and junction parameters are calculated. In the calibration phase there is no fluid over the sensor and no magnetic field. After this calibration phase a new phase begins for reading the sensors. In this subsequent phase the current is injected to the sensor structure and a magnetic field may also be applied. During the calibration and sensor measure, the temperature must be stabilized. The results are acquired using the high resolution ADC and pre-processed at the platform to be packed and sent to the PDA. In a full biochip reading this is repeated until all the  $M = 256$  sensors that compose the actual sensor matrix are read.

### 3.3. Communication and interface

Two types of communication can be used to control the platform: a wireless connection using the Bluetooth protocol or a USB connection.

The Bluetooth uses a full integrated class 2 module that has a maximum output power of  $2.5\text{ mW}$  and a typical range of  $20\text{ m}$ . The firmware supplied with this device offers a complete Bluetooth (v1.1) stack including profiles and command interface. It provides the Generic Access Profile (GAP), the Service Discovery Application Profile (SDAP), and the Serial Port Profile (SPP). This firmware features point-to-point and point-to-multipoint link management, supporting data rates up to the theoretical maximum of  $704\text{ kbps}$ . This module is linked to the peripheral control module via an Universal Asynchronous Receiver Transmitter (UART) interface.

For the USB, a microcontroller from Microchip, the PIC18F4550 that included a USB interface, was

adopted [8]. The current design will use the UART to send data to the Bluetooth module or to communicate directly with the analyser and the SPI to transfer between the SPM and the FCCM. The transmitted messages are parsed at the FCCM and then packed and send over a SPI connection to the SPM.

## 4. EXPERIMENTAL RESULTS

The proposed microsystem is presented in fig. 8. The biosensor array can be seen at the top of the board, and at the bottom the MC/DSP and the  $1\text{ Mbit}$  RAM chip.



Figure 8: Picture of the prototype: main board.

Measurements for noise levels in the main board were made using a sinusoidal current signal with a frequency of  $30\text{ Hz}$  and  $5\text{ }\mu\text{A}$  amplitude. The noise power spectral density can be seen in fig. 9. There are mostly four components in the noise: harmonics of the fundamental frequency ( $30\text{ Hz}$ ), quantization noise from the DAC,  $50\text{ Hz}$  power line frequency noise, low frequency noise, and white noise. The total noise level is about  $1\text{ mV}_{RMS}$ , due to DAC quantization. Together, power line and low frequency noise amount  $370\text{ }\mu\text{V}_{RMS}$ . If further data digital filtering is applied, the noise drops to about  $8\text{ }\mu\text{V}_{RMS}$ .

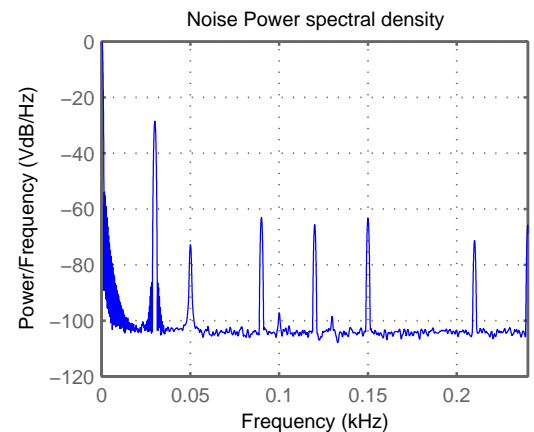


Figure 9: Noise power spectral density at the system.

The biochip is read by feeding two kinds of current values: a very small one,  $\approx 0.5 \mu A$ , for the DC voltage readings required to determine the temperature; and a higher current,  $10 \mu A$  or more, for particle detection. The biosensor current is controlled by the feedback loop shown in fig. 5. This loop was compensated and stabilized as can be seen in fig. 10 two sets of amplitude and phase curves are represented: (1-2) for current of  $10 \mu A$  and (3-4) for a biosensor current of  $0.5 \mu A$ . The amplitude and phase responses were obtained for the voltage gain measured between the collector of  $Q_{Sensor}$  and the voltage input, injected in the terminal of  $R_{Feed}$  connected to the ground in fig. 5. These experimental results show a very stable loop with a bandwidth larger than  $12 kHz$  for higher currents and enough bandwidth,  $700 Hz$ , for the DC temperature measures.

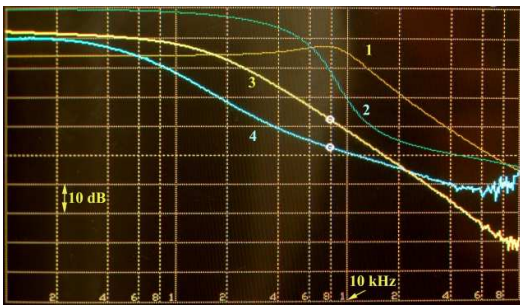


Figure 10: Frequency response of the current stabilization loop.

The microsystem was tested using a solution of  $2.3 \times 10^9$  particles/ml with  $1.5 \mu m$  diameter magnetic nanoparticles. A  $5 \mu A$  DC current was driven by the DAC through a  $10 k\Omega$  MTJ. The voltage signal was measured by an ADC at a sample rate of  $6 Hz$  after passing through a suitable anti-aliasing filter. The measurement time was about 8 minutes. The measured signal is presented in figure 11, after the removal of a  $47 mV$  DC signal. The solution was dropped on the sensor after acquiring about 1000 samples and after acquiring more 750 samples the sensor was washed with distilled water. The figure clearly shows a  $150 \mu V$  signal due to the presence of nanoparticles, demonstrating that the microsystem can be used for particle detection. The noise at the sensor could be further reduced by averaging. Also if the current level was increased to  $50 \mu A$  the signal level could be increased to  $300 \mu V$ , but this would lead to higher noise levels and lower signal to noise ratio.

## 5. CONCLUSIONS

This paper describes a new handheld microsystem architecture for biological analysis. The microsystem is based on a microchip with a matrix array of  $16 \times 16$  sensors, each one consisting on a diode in series with a MTJ, characterised in [6]. Experimental results show that the biosensor can be used for nanoparticle detection and, consequently, for magnetic label based bioassays. The

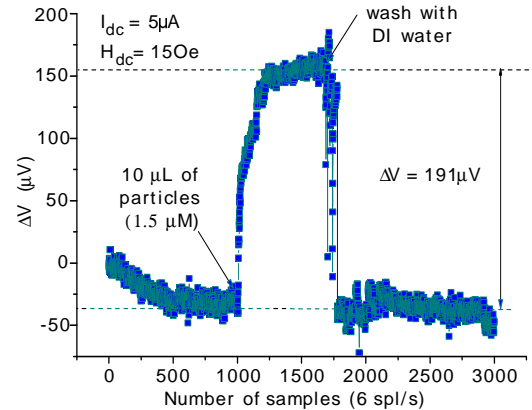


Figure 11: Time variation of the measured signal for evaluation of particle detection capabilities.

implemented microsystem, which is able to analyse data in real time, can be scaled in the future to accommodate matrix based biochips with up to 1000's biological probe sites.

## REFERENCES

- [1] O. Geschke, H. Klank, and P. Telleman, *Microsystems Engineering of Lab-on-a-chip Devices*. Wiley-VCH, 2004.
- [2] D. L. Graham, H. A. Ferreira, and P. P. Freitas, "Magnetoresistive-based biosensors and biochips: a review," *Trends Biotechnol.*, vol. 22, pp. 455–462, 2004.
- [3] M. Piedade, L. Sousa, J. Germano, J. Lemos, B. Costa, P. Freitas, H. Ferreira, F. A. Cardoso, and D. Vidal, "Architecture of a Portable System Based on a Biochip for DNA Recognition," in *Proc. of the XX conference on Design of Circuits and Integrated Systems*, 2005, ISBN 972-99387-2-5 (full paper in CD-ROM format).
- [4] V. C. B. Martins, L. P. Fonseca, H. A. Ferreira, D. L. Graham, F. A. Cardoso, J. Loureiro, J. Germano, L. Sousa, M. S. Piedade, B. A. Costa, J. M. Lemos, P. P. Freitas, and J. M. S. Cabral, "A magnetoresistive biochip for microbial analysis of water samples," in *LabAutomation2006*, 2006, in publication.
- [5] H. A. Ferreira, D. L. Graham, N. Feliciano, L. A. Clarke, M. D. Amaral, and P. P. Freitas, "Detection of Cystic Fibrosis Related DNA Targets Using AC Field Focusing of Magnetic Labels and Spin-Valve Sensors," *IEEE Trans. Magn.*, vol. 41.
- [6] T. M. A. *et al.*, "Magnetoresistive Biosensor Modelling for Biomolecular Recognition," in *XVIII IMEKO WORLD CONGRESS*, 2006, in publication.
- [7] "High Performance Digital Signal Controllers - dsPIC30F3010 DataSheets," Microchip, 2005.
- [8] "PIC18F2455/2550/4455/4550 Data Sheet," Microchip, 2004.